Supplementary Methods

The behavior of the single-neuron HVC_{RA} model in response to depolarizing and hyperpolarizing current pulses is shown in Fig. S1A-C (cf. Kubota and Taniguchi 1998, Fig. 2A1,C,D). The behavior of the HVC_I model is shown in Fig. S1D-F (cf. Kubota and Taniguchi 1998, Fig. 3A,C,D; and Dutar et al. 1998, Fig. 1C).

In the simulations shown in Fig. S1, we divided the injected current by an assumed effective membrane surface area. We adjusted the effective membrane surface area solely to adjust the input resistance and thereby scale the frequency-current relationships in this supplementary figure to match the data of Kubota and Taniguchi (1998). These effective membrane surface areas are not based on experimental data; however, they did not play a role in our network simulations because we expressed all ionic currents per unit surface area and adjusted maximal synaptic conductances to achieve the desired network behavior. In other words, a decrease in surface area can be compensated by an increase in synaptic strength, and vice versa. We assumed an effective membrane surface area of 2400 μm^2 for the HVC_{RA} neuron and 12500 μm^2 for the HVC_I neuron in this figure.

Supplementary Results

In Fig. S3A, we demonstrate bistability in a 3-HVC_{RA} reduced cluster model without an HVC_I neuron and with g_{AMPA} = 1.2 mS/cm^2. In the absence of input, the cluster will remain in its quiescent state indefinitely. By exciting HVC_{RA} neuron 1 of the cluster with a 3 ms, 50 $\mu A/cm^2$

DC current pulse beginning at t = 10 ms (green arrow), we shift the cluster into its persistently spiking state. We then shift the cluster back into its quiescent state with a 3 ms, -50 μA/cm^2 current pulse into the same neuron beginning at t = 110 ms (red arrow).

In our model, each HVC_{RA} neuron sends an excitatory synapse to, and receives an inhibitory synapse from, the HVC_I neuron (Fig. 3A). In Fig. S3B, we show the behavior of neurons in a cluster with g_{AMPA} = 1.2 for $HVC_{RA} \rightarrow HVC_{RA}$ synapses, g_{AMPA} = 0.1 for $HVC_{RA} \rightarrow HVC_I$ synapses, and g_{GABAA} = 0.8 for $HVC_I \rightarrow HVC_{RA}$ synapses. We again excite neuron 1 with a 3 ms, 50 μA/cm^2 current pulse beginning at t = 5 ms. The stimulated neuron (Fig. S3B, top; blue trace) then excites the other two HVC_{RA} neurons (Fig. S3B, top; green and red traces) and the HVC_I neuron (Fig. S3B, bottom). The HVC_I neuron in turn terminates the activity of the HVC_{RA} neurons after each spikes 2 to 4 times, in 6.8 ± 2.1 ms.

Supplementary Figure Legends

FIG. S1. Intrinsic properties of HVC_{RA} and HVC_I model neurons at 32°C. *A:* Plots of spiking frequency vs. time at different current amplitudes for our model HVC_{RA} neuron (cf. Kubota and Taniguchi 1998, Fig. 2D). *B:* Response of the HVC_{RA} neuron to a 300 ms, 0.09 nA depolarizing current pulse (cf. Kubota and Taniguchi 1998, Fig. 2C). *C:* Response of the HVC_{RA} neuron to a 300 ms, -0.06 nA hyperpolarizing current pulse (cf. Kubota and Taniguchi 1998, Fig. 2A1). *D:* Plots of spiking frequency vs. time at different current amplitudes for our model HVC_I neuron (cf. Kubota and Taniguchi 1998, Fig. 3D). *E:* Response of the HVC_I neuron to a 300 ms, 0.70 nA depolarizing pulse *(top)* (cf. Kubota and Taniguchi 1998, Fig. 3C and Dutar et al. 1998, Fig. 1C1). *F:* Response of the HVC_I neuron to a 300 ms, -0.50 nA hyperpolarizing pulse *(bottom)* (cf. Kubota and Taniguchi 1998, Fig. 3A and Dutar et al. 1998, Fig. 1C2).

FIG. S2. Burst duration for the inhibitory pause mechanism of Fig. 1C as a function of various parameters. *Dark gray lines:* mean ± SD. *Light gray regions:* HVC_{RA} burst duration (mean ± SD) measured by Kozhevnikov and Fee (2007). Note that this mechanism is less sensitive to parameter changes than the inhibitory buildup mechanism is (cf. Fig. 2). *A:* Inhibitory synaptic decay time constant, $1/\beta$ (normal value: 5.6 ms). *B:* Inhibitory synapses per HVC_I, normal adaptation currents present (normal number: 70). *C:* Scale factor by which the maximal conductances of both adaptation currents are multiplied (normal value: 1). *D:* Inhibitory synapses per HVC_I, adaptation currents absent. *E:* Excitatory synapses per HVC_{RA} (normal number: 80).

FIG. S3. *A:* Bistability of the 3-HVC_{RA} reduced cluster model without an HVC_I neuron. *Green arrow:* time of excitatory current pulse. *Red arrow:* time of inhibitory current pulse. *B:* When the $HVC_I \rightarrow HVC_{RA}$ synapses are of an appropriate strength, the HVC_{RA} neurons show a brief burst of activity. *Top:* Response of a cluster of three HVC_{RA} neurons to a 3 ms, 50 $\mu A/cm^2$ current pulse injected into HVC_{RA1} (*blue trace*), beginning at t = 5 ms. When HVC_{RA1} is excited, it excites HVC_{RA2}, (*green*), HVC_{RA3} (*red*), and HVC_I (*bottom)*. The HVC_I neuron terminates the spiking of the HVC_{RA} neurons.

FIG. S4. Raster plot of the spike times in a chain of 20 clusters with physiological synaptic strengths. This plot illustrates the propagation of activity along the HVC_{RA} network, the consistency of burst duration, and the sustained activity of HVC_I neurons. A cluster contains 80 HVC_{RA} neurons, each of which sends a single AMPA synapse to each of 40 other HVC_{RA} neurons in its cluster, 40 in the previous cluster, and 40 in the next cluster. Each of the 1600 HVC_I neurons receives an AMPA synapse from each of 20 HVC_{RA} neurons and sends a $GABA_A$ synapse to each of 80 HVC_{RA} neurons, and is constrained not to send inhibition within 10 clusters downstream, or 1 cluster upstream, of one from which it receives excitation. We initiated spiking in the first cluster with a 4 ms, 40 $\mu A/cm^2$ DC current pulse in 50% of the HVC_{RA} neurons, beginning at t = 0 ms.

FIG. S5. Blocking $GABA_A$ receptors reduces the sparseness of HVC_{RA} bursting. Raster plot of spike times of a subset of HVC_{RA} and HVC_I neurons from a simulation of 90 HVC_I neurons and 60 clusters of 3 HVC_{RA} neurons, in which the inhibitory maximal conductance, g_{GABAA}, was set to zero. Each HVC_{RA} burst began normally but failed to terminate, thus showing persistent activity. We set the threshold for determining spike time at -30 mV to catch low-amplitude spikes in the HVC_I neurons.

FIG. S1

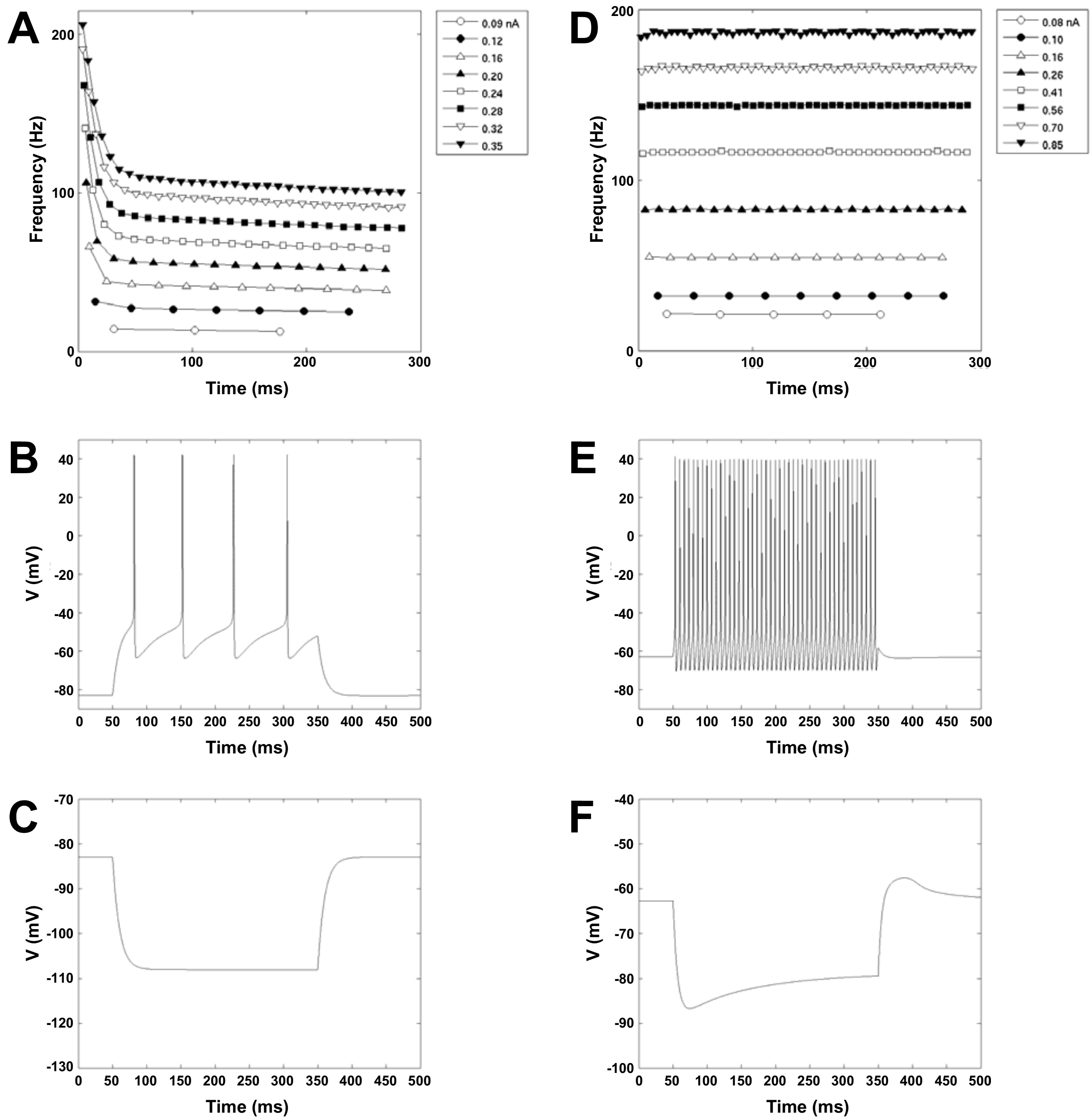

A
Frequency (Hz)
Time (ms)
0.09 nA
0.12
0.16
0.20
0.24
0.28
0.32
0.35
D
Frequency (Hz)
Time (ms)
0.08 nA
0.10
0.16
0.26
0.41
0.56
0.70
0.85
B
V (mV)
Time (ms)
E
V (mV)
Time (ms)
C
V (mV)
Time (ms)
F
V (mV)
Time (ms)

FIG. S2

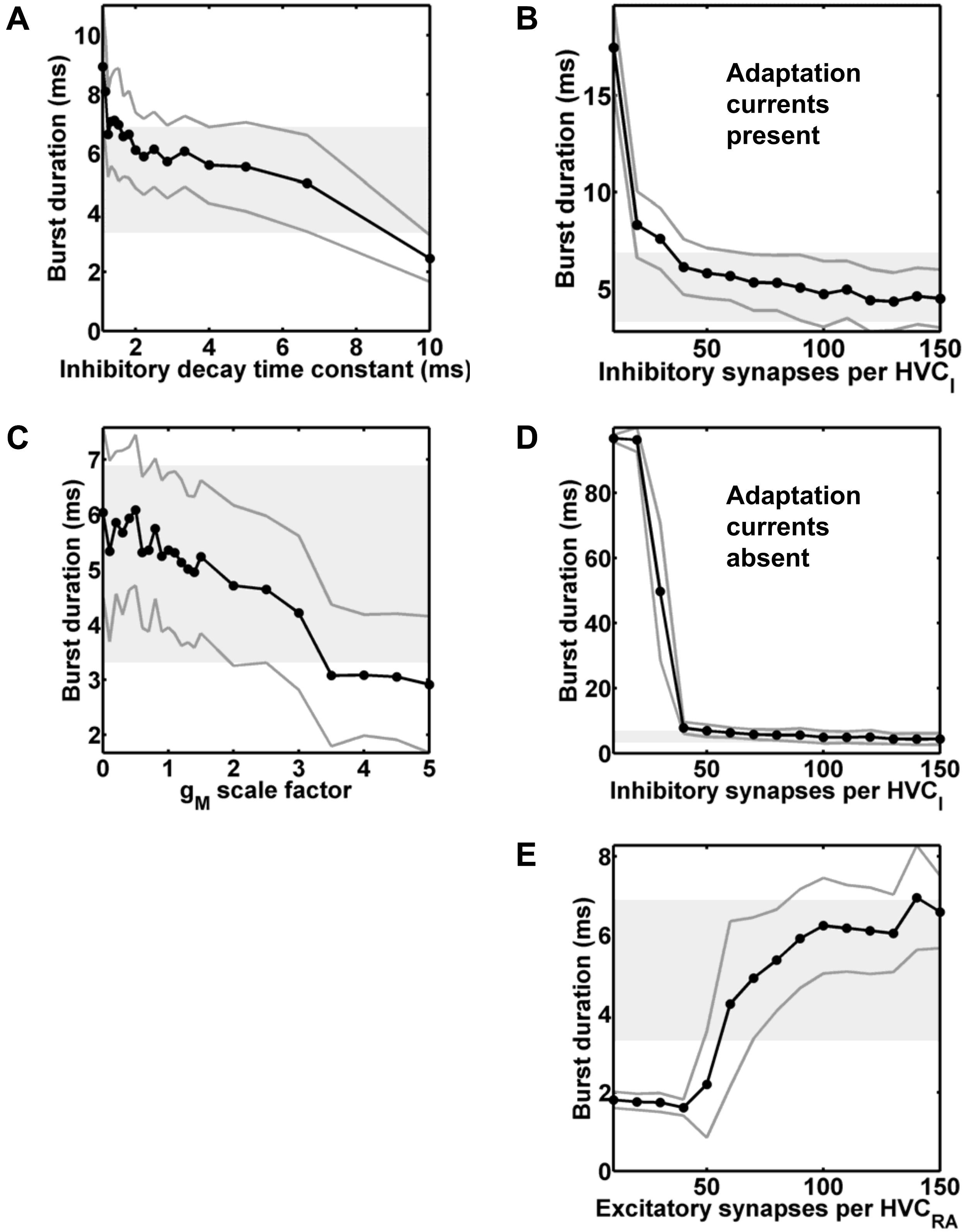

A
Burst duration (ms)
Inhibitory decay time constant (ms)
B
Adaptation currents present
Burst duration (ms)
Inhibitory synapses per HVC_I
C
Burst duration (ms)
g_M scale factor
D
Adaptation currents absent
Burst duration (ms)
Inhibitory synapses per HVC_I
E
Burst duration (ms)
Excitatory synapses per HVC_RA

FIG. S3

3-HVC_{RA} cluster:

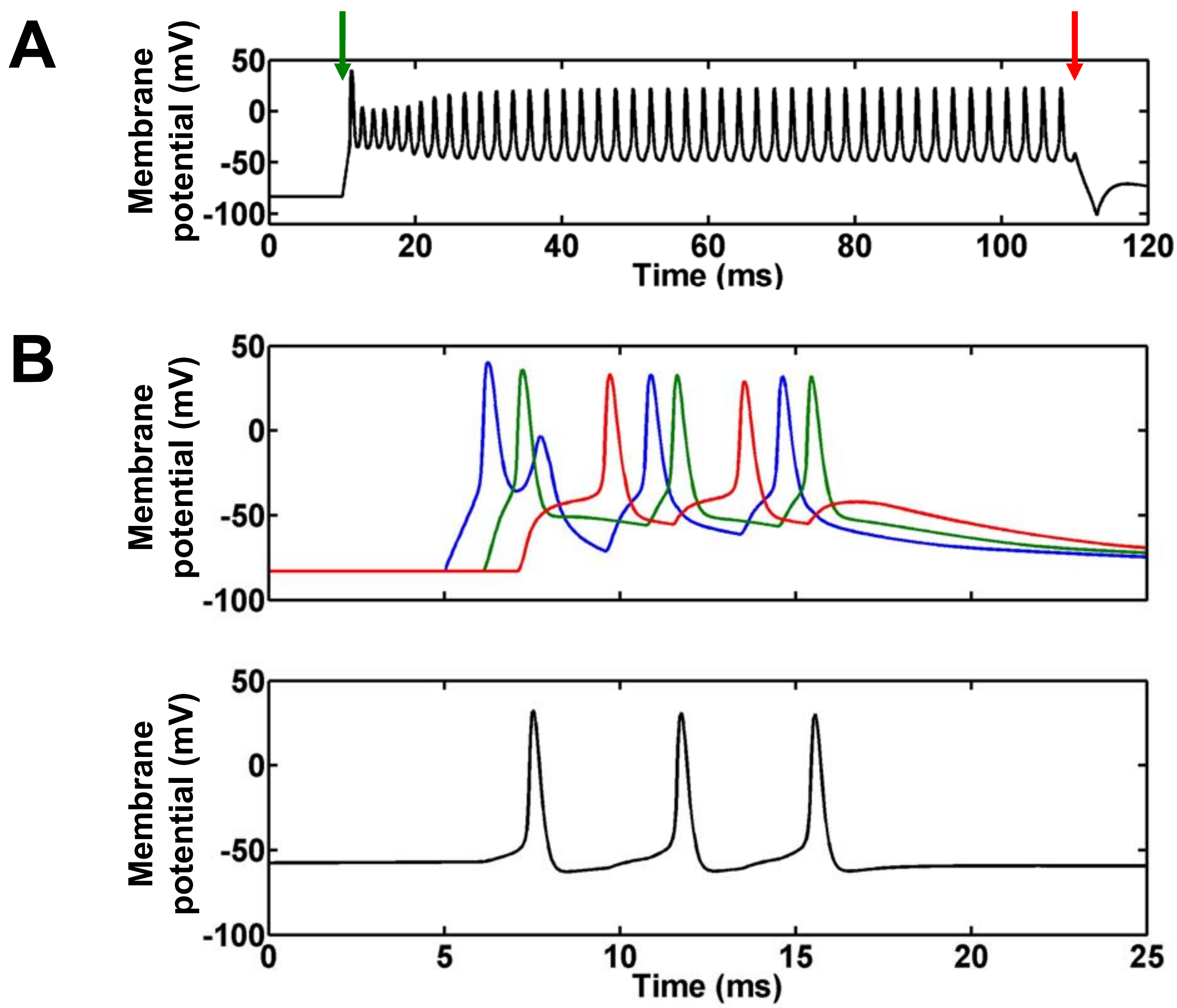

FIG. S4

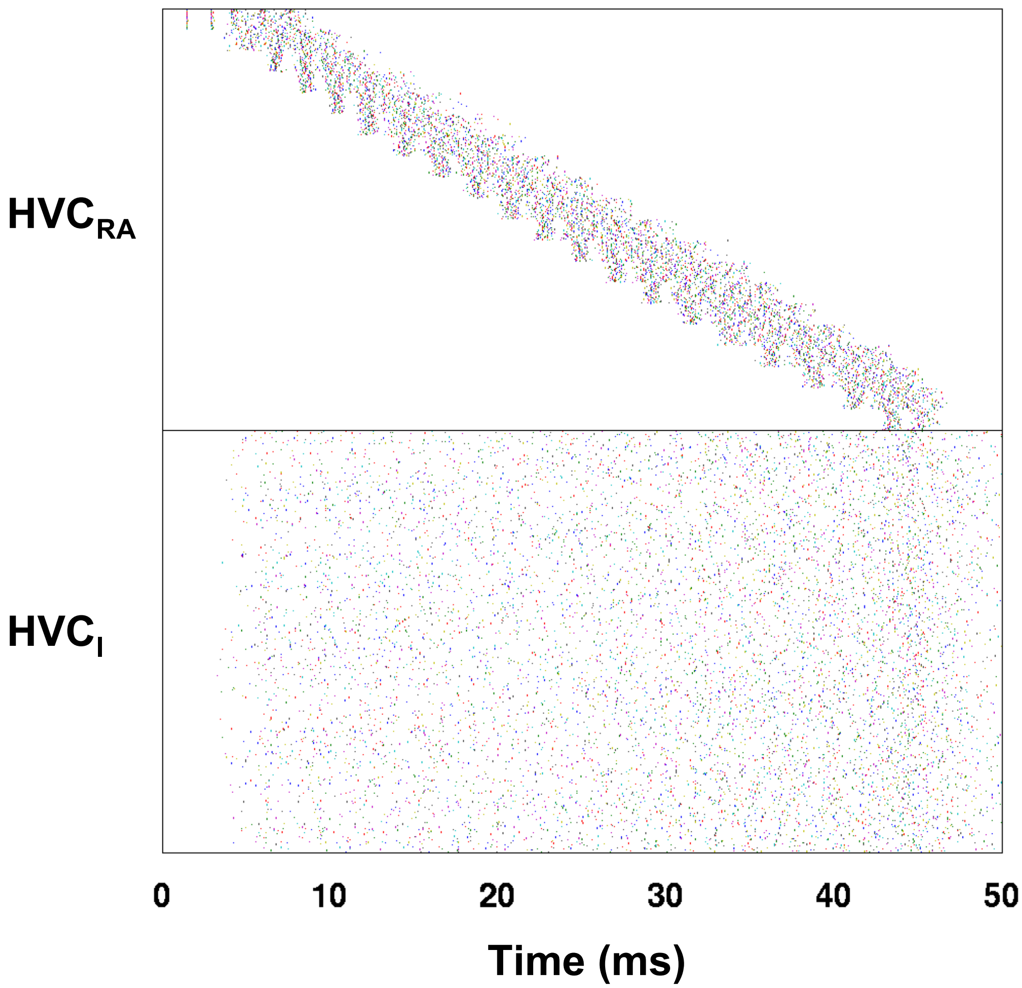

FIG. S5